Electrochemistry Communications 115 (2020) 106739

Contents lists available at ScienceDirect

Electrochemistry Communications

journal homepage: www.elsevier.com/locate/elecom

Electrochemical copper dissolution: A benchmark for stable CO_2 reduction on copper electrocatalysts

Florian D. Speck[a,b,*], Serhiy Cherevko[a,*]

[a] Forschungszentrum Jülich GmbH, Helmholtz Institute Erlangen-Nürnberg for Renewable Energy (IEK-11), Egerlandstr. 3, 91058 Erlangen, Germany
[b] Department of Chemical and Biological Engineering, Friedrich-Alexander-Universität Erlangen-Nürnberg, Egerlandstr. 3, 91058 Erlangen, Germany

ARTICLE INFO

Keywords:
CO_2 reduction
Copper
Dissolution
Stability
ICP–MS

ABSTRACT

Copper is well known in fundamental electrocatalysis research due to its ability to selectively reduce CO_2 to C_2 products. Recent, more applied studies have revealed that electrolyzers based on Cu electrocatalysts can reach current densities of up to hundreds of mA cm^{-2}. This opens up the opportunity for industrial application of Cu-based electrocatalysts. However, the stability of copper must first be assessed. In this communication we investigate the electrochemical corrosion behavior of copper in a broad pH window relevant to CO_2 reduction applications. Using an electrochemical on-line inductively coupled plasma mass spectrometer (ICP-MS), we quantify Cu dissolution during anodic oxidation and during the reduction of electrochemically formed oxide species. We show that electrochemical oxidation of Cu leads to high dissolution in neutral and highly alkaline environments, while an intermediate pH of around 9–10 leads to minimal dissolution. The obtained results are discussed in relation to the CO_2 reduction reaction to set a benchmark for stable Cu-based electrocatalysts.

1. Introduction

Copper is the noblest of the 3d transition metals. Depending on potential, it can form two stable passivating oxides at neutral pHs [1]. Combined with other attributes, e.g. high electrical conductivity, these properties make Cu a valuable material for many industrial applications. In electrocatalysis, Cu has received growing attention due to its ability to selectively reduce carbon dioxide to C_2 species like ethylene in the electrochemical CO_2 reduction reaction (CO_2RR) [2–6]. With the recent development of coupled electrochemical techniques, it has become possible to unravel the complex assortment of products generated during the CO_2RR [3,5,6]. Interestingly, these techniques have also revealed that the previous history and pretreatment of the electrode can have a significant impact on CO_2RR product composition [5–9]. The most prominent explanations include the formation of favorable crystal facets [4,10–13], grain boundary effects [7], and the existence of subsurface oxygen [14,15]. The latter has been hypothesized to influence the electronic parameters of the top Cu monolayer and, hence, the energy of adsorption of the CO_2RR intermediates [15]. To fully understand the changes on the Cu surface during electrode pretreatment and their effect on CO_2RR selectivity, possible Cu dissolution must also be considered. Interestingly, while it is now well known that noble metals are prone to dissolve during the surface oxidation/reduction, Cu dissolution has not yet been addressed in detail. Reports on Cu dissolution in strong alkaline and acidic electrolyte from the perspective of fundamental research can be found, but these rarely reflect on operating conditions for CO_2 electrocatalysis [16–20].

Data on Cu dissolution are deemed necessary to design accelerated stress tests (AST) for unified stability testing in the academic community [21]. According to thermodynamic considerations by M. Pourbaix, Cu corrodes in acidic and highly alkaline environments [1]. While fundamental CO_2RR investigations are generally conducted in neutral carbonate buffers, some considerations of local pH changes at the electrode in operando conditions are necessary. Previous studies have revealed that due to the hydrogen evolution reaction (HER) and the consumption of protons during CO_2RR, Cu can experience local pHs of up to 13 [22,23]. Thus, high current densities will lead to the rapid depletion of protons at the surface and a significant increase in pH [23]. From this consideration it follows that a combination of high pH and anodic potential, e.g. during cell off periods, may lead to Cu dissolution.

In the following we investigate the corrosion of copper in the neutral to alkaline pH range. We quantify Cu dissolution using an electrochemical scanning flow cell (SFC) connected on-line to an inductively coupled plasma mass spectrometer (ICP–MS) and show that dissolution is lowest at pH 9–10. Tracking the onset of Cu dissolution, we demonstrate that dissolution is caused by transitions in the Cu

* Corresponding authors at: Forschungszentrum Jülich GmbH, Helmholtz Institute Erlangen-Nürnberg for Renewable Energy (IEK-11), Egerlandstr. 3, 91058 Erlangen, Germany (F.D. Speck).
E-mail addresses: f.speck@fz-juelich.de (F.D. Speck), s.cherevko@fz-juelich.de (S. Cherevko).

https://doi.org/10.1016/j.elecom.2020.106739
Received 9 April 2020; Received in revised form 23 April 2020; Accepted 26 April 2020
Available online 29 April 2020

oxidation state. The results are discussed with specific regard to the application of Cu in CO_2RR applications.

2. Experimental

All electrochemical corrosion investigations were carried out on a polycrystalline Cu foil (Alfa Aesar, 99.9999% metal basis) which was ground (SiC paper 500, 2000 and 4000 grid) and polished (MD mol, 3 μm) thoroughly using a polishing machine (Struers, LaboForce-100). Using a laser profilometer (Keyence, VK-X250), the roughness factor was estimated to be 1.01. An inductively coupled plasma mass spectrometer (ICP–MS, Perkin Elmer, NexION 350×) was used for *in-situ* detection of dissolved Cu species by coupling it to the electrolyte outlet of a custom polycarbonate scanning flow cell (SFC). On the inlet (angled at 60° to the outlet) the SFC was connected to a graphite counter electrode (Sigma Aldrich, 99.995% trace metal basis). A third capillary channel connected a reference electrode (Metrohm, Ag/AgCl) closely to the working electrode surface. Contact of the cell with the working electrode was made with a xyz-translation stage (Physik Instrumente), while the potential was controlled with 90% iR correction using a potentiostat (Gamry, Reference 600). The flow rate of the Ar purged electrolytes was set at 220 μL min^{-1} using the peristaltic pump of the ICP–MS (Elemental Scientific, MP2 Pump). In the following, both the raw dissolution data (grey circles) and the smoothed traces (solid colors) are presented. For further information on the experimental setup, please refer to Fig. S1 and our previous reports [24]. Five electrolytes with different pH values were prepared. An unbuffered KOH (Sigma-Aldrich, 99.99%) electrolyte was prepared by dissolving KOH in water (Merck, MilliQ®, 18.2 MΩ) to 0.05 M. Phosphate-buffered electrolytes with pH values of 12, 10, 8, 6.8 were prepared from a 0.05 M (KH_2PO_4/K_2HPO_4, Meck, Suprapur®) buffer solution. KOH was added until the desired pH was reached. The pH of all electrolytes was measured (Mettler Toledo, SevenExcellence™) just before the experiments. All error bars are taken from at least two independent measurements.

3. Results and discussion

Potential-dependent dissolution of copper was studied by tracking the concentration of dissolved Cu in the electrolyte using on-line ICP-MS. First, cyclic voltammograms (CV) on a pretreated copper electrode (Supplementary Information, Section 2) were recorded in a positive potential window vs. the reversible hydrogen electrode (RHE) (Fig. 1A). Fig. 1B shows a typical Cu oxidation/reduction CV profile, which consists of at least two anodic, a^I and a^{II}, and two cathodic, c^I and c^{II}, peaks. The copper dissolution profile shown in Fig. 1C correlates well with the redox processes observed in the CV. Upon oxidation to Cu^I (a^I) at 0.5 V_{RHE}, a transient Cu dissolution peak occurs followed by a second more intense dissolution peak at 0.78 V_{RHE} during the transition to Cu^{II} (a^{II}). However, during the reduction back to Cu^I (c^{II}) only a minor dissolution peak occurs at 0.66 V_{RHE}. The dissolution rate during further reduction to Cu^0 (c^I) is only observed as a minor tail of the previous dissolution event. A lack of further dissolution at such low potentials could be due to redeposition of dissolved species as metallic Cu. Once full reduction is achieved, the dissolution quickly moves back to the baseline, indicating that Cu is not broken down at these potentials. Furthermore, an experiment at negative potentials has shown that Cu is immune towards dissolution down to −1 V_{RHE} but further oxidation at open circuit potential results in dissolution (Supplementary Information, Fig. S3).

The clear correlation between oxidation/reduction and dissolution processes in Fig. 1 was investigated further, with the results summarized in Table 1. The experimental onset potentials of dissolution (E_{on}) were determined as the potentials at which the ICP-MS signal surpasses three times the standard deviation of the baseline signal. Standard thermodynamic potentials (E_{th}) for Cu oxidation and reduction processes [1], highlighted in Fig. 1A, are also included in Table 1. The difference (ΔE)

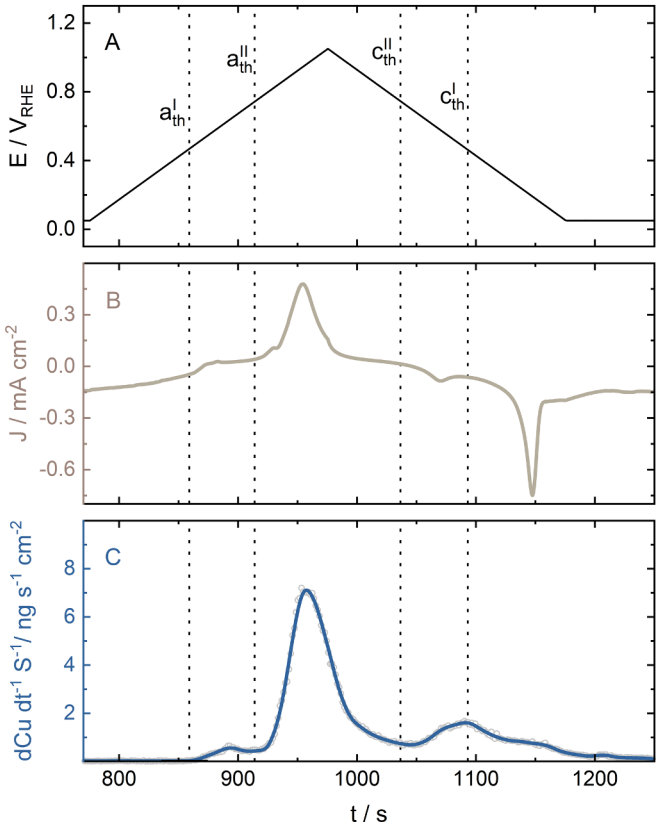

Fig. 1. On-line ICP-MS data of copper during a CV between 0.05 and 1.05 V_{RHE} at 5 mV s^{-1} in 0.05 KOH. The panels show (A) the potential together with the thermodynamic potentials of Cu to Cu_2O and CuO transitions during oxidation ($a^{I,II}_{th}$) and reduction ($c^{I,II}_{th}$) as well as (B) the experimental current density and (C) the Cu dissolution rate on the same time axis.

between E_{on} and E_{th} was used as a metric for correlation between the redox and dissolution processes. Positive and negative ΔE values for anodic and cathodic processes, respectively, have implications for dissolution overpotentials. As the ΔE values are relatively low, we can conclude that Cu dissolution is a transient process initiated by surface restructuring during oxidation/reduction. Similar correlations were observed for other noble metals in acidic and alkaline electrolytes [25,26]. The dissolution peaks are also shifted slightly with respect to the corresponding redox peaks, which is related to dissolution peak spreading [27].

The amount of dissolved Cu in each process was obtained by integration of the corresponding dissolution peaks. Moreover, in order to estimate the dissolution selectivity, the individual integrals of the CV peaks were obtained as the charges passed (Q_{pass}). Since ICP-MS does not provide information on the oxidation state of dissolved Cu ions, an arbitrary oxidation state identical to the corresponding oxide was chosen. While during both anodic transitions around 4–7% of the current is due to Cu dissolution, there is a distinct difference between the two cathodic transitions. During the reduction from Cu^{II} to Cu^I more than 15% of the reduction charge is caused by Cu dissolution. The transition from Cu^I to Cu^0 occurs with only minor dissolution of ca. 1%, possibly due to redeposition at low potentials. The overall amount of Cu dissolved within one CV is ca. 523 ± 1 ng cm^{-2}, which corresponds to 3.25 monolayers of metallic Cu.

Next we compare the anodic and cathodic currents. From Table 1, there is a minor discrepancy between anodic and cathodic charges during a CV, leaving a surplus of 0.8 ± 0.2 mC cm^{-2} of anodic charge. Such a surplus could be interpreted as residual subsurface Cu oxides. If we consider the corresponding anodically dissolved amount of Cu

Table 1
Cu dissolution in 0.05 KOH with key indicators.

	E_{th} [V_{RHE}]	E_{on} [V_{RHE}]	ΔE [mV]	Q_{pass} [mC cm^{-2}]	Dissolved Cu [ng cm^{-2}]	%[a]
a^I	0.471	0.497 ± 4 mV	26 ± 4	0.86 ± 0.04	22.4 ± 1	4 ± 0.02
a^{II}	0.747	0.783 ± 3 mV	36 ± 3	7.51 ± 0.84	352.5 ± 5	7.2 ± 0.7
c^{II}	0.747	0.660 ± 1 mV	−87 ± 1	0.98 ± 0.05	100.2 ± 4	15.5 ± 1.4
c^I	0.471	n.r.[b]	n.r.	6.58 ± 0.98	47.6 ± 1	1.1 ± 0.2

[a] see SI; [b] not resolved.

(375 ± 6 ng cm^{-2}) and calculate the charge that it took to oxidize to the dissolved species (0.6 ± 0.01 mC cm^{-2}), we get a difference of only 0.2 ± 0.2 mC cm^{-2} between anodic and cathodic charges. (For further details see Supplementary Information, section 2.) This is within the error of integration and we therefore propose that during the Cu^I/Cu^0 reduction most subsurface oxide can be reduced, accompanied by minor cathodic dissolution. Therefore our findings do not coincide well with the assumption of subsurface oxygen [15], similar to recent literature where DFT shows the poor stability of subsurface oxygen [28], and O^{18} labeling experiments demonstrated the disappearance of oxygen upon reduction (< 1%) [29]. On the other hand, the significant anodic and cathodic dissolution of 3.25 monolayers within just one cycle supports the hypothesis of crystal facet modification during the anodic/cathodic treatment. While there is no data on dissolution of Cu single crystals, dissolution of an f.c.c. lattice should increase with decrease in atomic coordination number (1 1 1) > (1 0 0) ≫ (1 1 0). The latter was recently shown for Pt [30,31]. Assuming that there is indeed preferential leaching of less coordinated Cu atoms, selective formation of C_2 products on anodically treated Cu could be caused by (1 1 1) texturing of the surface. This is in line with recent findings on CO_2RR on Cu single crystals [10]. For further insight on this effect, dissolution studies similar to those on Pt single crystals by Sandbeck et al. [30] would be necessary on single crystalline Cu.

To expand the Cu stability investigations to a pH regime relevant for CO_2RR, we conducted additional CV experiments in various phosphate-buffered electrolytes. Note, the use of commonly investigated carbonate buffers that require CO_2 purging proved unviable in the SFC due to bubble formation in the small diameter tubing. However, we believe that pH is the governing factor in Cu dissolution stability, since both anions (carbonate and phosphate) should complex Cu ions similarly. Fig. 2A shows the dissolution rate of Cu at pH 12, 10, 8 and 6.8, while Fig. 2B depicts the dissolved amount of Cu. A simplified scheme of the Cu Pourbaix diagram relevant to the following discussion is shown in Fig. 2C. In Fig. 2A, it becomes unambiguously clear that the rate of Cu dissolution increases during oxidation, when the pH becomes that of the thermodynamically favored aqueous species of Cu (Cu^{2+} acidic, $HCuO_2^-$ alkaline). At pH = 6.8, the pH of the commonly used carbonate buffer in CO_2RR half-cell testing, the anodic polarization forces Cu significantly inside the dissolution regime. Furthermore, for pH 6.8 and 12, high potentials (> 1.4 V_{RHE}) lead to the oxygen evolution reaction (OER) on Cu. Thus an additional OER dissolution peak, on top of the transient dissolution plateau, is observed here [32,33]. Such high potentials are of special interest in the electrochemical preconditioning of Cu [5,15].

To explain the effect of pH on the extent of dissolved copper, we need to consider the pH dependence of the thermodynamic transitions. The stability window of the solid oxide species, Cu_2O and CuO, is dependent on the concentration of dissolved Cu species. Therefore, the further the pH deviates from the center of this stability window (thermodynamically at pH 8.91 [1]), the higher the concentration of dissolved species can become before passivation occurs. In short, the passivating effect of the oxide layer only inhibits transient dissolution at pH values close to 9.

These considerations are vital to CO_2RR research in many ways. On the one hand, mechanistic studies should consider dissolved Cu species

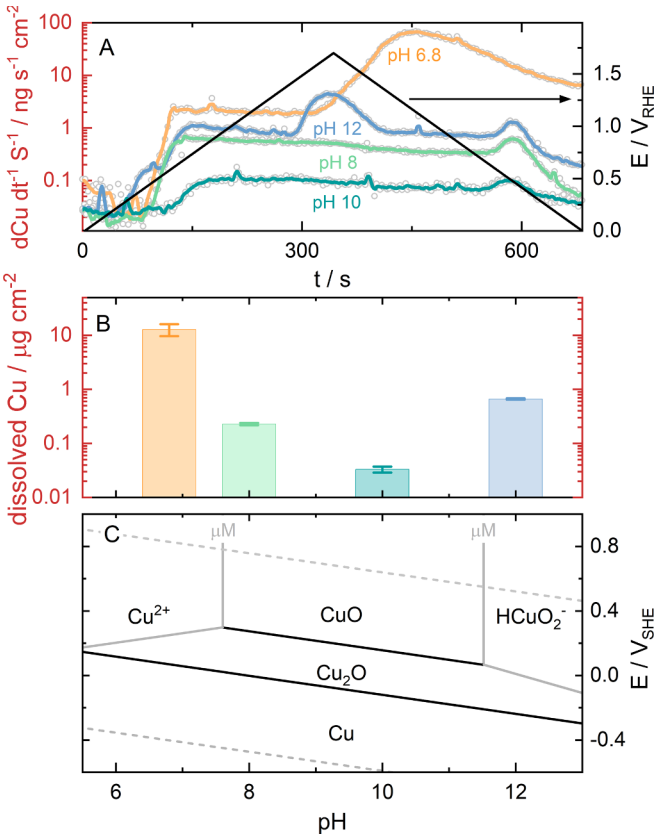

Fig. 2. (A) Dissolution rate of Cu during a single CV from 0 to 1.6 V_{RHE} at 5 mV s^{-1} in phosphate-buffered electrolytes ranging from pH 12 to 6.8. (B) Integrals of Cu dissolution during CVs from (A). (C) A simplified pH region of the Cu Pourbaix diagram (solid), equilibrium reactions of water (dashed).

in the electrolyte if an anodic treatment is applied, and the effect of crystal facet stability trends and pH dependence of dissolution should give important insights into activity and selectivity improvements. On the other hand, moving towards application of Cu as a possible electrocatalyst in real devices, start/stop conditions have to be considered and AST protocols need to be defined [21]. In general, operation at low potentials and high local pH will not lead to dissolution, although other degradation processes must not be overlooked. A shutdown, however, may cause a slow decrease in the local pH from the working conditions (12–14) to the bulk pH of roughly 7 and a high anodic open circuit potential, oxidizing and dissolving the catalyst. By contrast, the startup of the oxidized catalyst will lead to full reduction, accompanied by additional dissolution as well as catalyst surface reconstruction. Lastly, the dissolved copper in the electrolyte could cause system-wide problems, since it can deposit in membranes and other components, similar to iridium in water electrolysis systems and platinum in hydrogen fuel cells [34]. Considerations like these are imperative for future work on Cu electrocatalysts for the CO_2RR, especially under high current working conditions. Dissolution needs to be addressed in real devices and the effects of the anions present, like carbonates, need to be re-

evaluated to consider possible complexing behavior and its effect on dissolution.

4. Conclusion

This on-line ICP-MS study revealed that Cu dissolves transiently during its surface oxidation and reduction. The extent of dissolution depends on pH, with the highest stability being observed at pH 9–10. Further, by accounting for dissolution, the total Cu oxidation and reduction charges were balanced. This finding implies that it is unlikely that subsurface oxygen remains after the full reduction of electrochemically formed CuO_x. Besides the amounts, the onsets of Cu dissolution were also estimated, thus defining the experimental stability window of Cu. This set of new data establishes a baseline for the stable operation of CO_2RR electrolyzers. Our results imply that in order to minimize Cu dissolution, the potential should not exceed the Cu^0/Cu^I couple. In cases where this is difficult to avoid, the local pH should be close to 10. Hence, management of both potential and pH is essential for long-term stability of Cu-based CO_2RR electrocatalysts. These data, together with detailed information on potential and pH changes in real devices, will assist in the development of accelerated stress tests for Cu-based CO_2RR electrocatalysts.

CRediT authorship contribution statement

Florian D. Speck: Investigation, Visualization, Writing - original draft. **Serhiy Cherevko:** Supervision, Validation, Writing - review & editing.

Declaration of Competing Interest

The authors declare that they have no known competing financial interests or personal relationships that could have appeared to influence the work reported in this paper.

Appendix A. Supplementary data

Supplementary data to this article can be found online at https://doi.org/10.1016/j.elecom.2020.106739.

References

[1] M. Pourbaix, Atlas of Electrochemical Equilibria in Aqueous Solutions, NACE International, 1974.

[2] L. Wang, S.A. Nitopi, E. Bertheussen, M. Orazov, C.G. Morales-Guio, X. Liu, D.C. Higgins, K. Chan, J.K. Nørskov, C. Hahn, T.F. Jaramillo, Electrochemical carbon monoxide reduction on polycrystalline copper: Effects of potential, pressure, and pH on selectivity toward multicarbon and oxygenated products, ACS Catal. 8 (2018) 7445–7454.

[3] J.-P. Grote, A.R. Zeradjanin, S. Cherevko, A. Savan, B. Breitbach, A. Ludwig, K.J.J. Mayrhofer, Screening of material libraries for electrochemical CO_2 reduction catalysts – improving selectivity of Cu by mixing with Co, J. Catal. 343 (2016) 248–256.

[4] J. Hussain, H. Jónsson, E. Skúlason, Calculations of product selectivity in electrochemical CO_2 reduction, ACS Catal. 8 (2018) 5240–5249.

[5] P. Khanipour, M. Loffler, A.M. Reichert, F.T. Haase, K.J.J. Mayrhofer, I. Katsounaros, Electrochemical real-time mass spectrometry (EC-RTMS): monitoring electrochemical reaction products in real time, Angew. Chem. Int. Ed. 131 (2019) 7351–7355.

[6] L. Mandal, K.R. Yang, M.R. Motapothula, D. Ren, P. Lobaccaro, A. Patra, M. Sherburne, V.S. Batista, B.S. Yeo, J.W. Ager, J. Martin, T. Venkatesan, Investigating the role of copper oxide in electrochemical CO_2 reduction in real time, ACS Appl. Mater. Interfaces 10 (2018) 8574–8584.

[7] C.W. Li, M.W. Kanan, CO_2 reduction at low overpotential on Cu electrodes resulting from the reduction of thick Cu_2O films, J. Am. Chem. Soc. 134 (2012) 7231–7234.

[8] M. Le, M. Ren, Z. Zhang, P.T. Sprunger, R.L. Kurtz, J.C. Flake, Electrochemical reduction of CO_2 to CH_3OH at copper oxide surfaces, J. Electrochem. Soc. 158 (2011) E45–E49.

[9] B.P. Sullivan, K. Krist, H.E. Guard (Eds.), Electrochemical and Electrocatalytic Reactions of Carbon Dioxide, 1st ed., Elsevier Science, 1992.

[10] K.J.P. Schouten, Z. Qin, E. Pérez Gallent, M.T.M. Koper, Two pathways for the formation of ethylene in co reduction on single-crystal copper electrodes, J. Am. Chem. Soc. 134 (2012) 9864–9867.

[11] Y. Hori, I. Takahashi, O. Koga, N. Hoshi, Electrochemical reduction of carbon dioxide at various series of copper single crystal electrodes, J. Mol. Catal. A Chem. 199 (2003) 39–47.

[12] R.M. Arán-Ais, F. Scholten, S. Kunze, R. Rizo, B. Roldan Cuenya, The role of in situ generated morphological motifs and Cu(I) species in C_{2+} product selectivity during CO_2 pulsed electroreduction, Nat. Energy 5 (2020) 317–325.

[13] Y.G. Kim, J.H. Baricuatro, A. Javier, J.M. Gregoire, M.P. Soriaga, The evolution of the polycrystalline copper surface, first to Cu(111) and then to Cu(100), at a fixed CO(2)RR potential: a study by operando EC-STM, Langmuir 30 (2014) 15053–15056.

[14] H. Mistry, A.S. Varela, C.S. Bonifacio, I. Zegkinoglou, I. Sinev, Y.W. Choi, K. Kisslinger, E.A. Stach, J.C. Yang, P. Strasser, B.R. Cuenya, Highly selective plasma-activated copper catalysts for carbon dioxide reduction to ethylene, Nat. Commun. 7 (2016) 12123.

[15] A. Eilert, F. Cavalca, F.S. Roberts, J. Osterwalder, C. Liu, M. Favaro, E.J. Crumlin, H. Ogasawara, D. Friebel, L.G. Pettersson, A. Nilsson, Subsurface oxygen in oxide-derived copper electrocatalysts for carbon dioxide reduction, J. Phys. Chem. Lett. 8 (2017) 285–290.

[16] H.H. Strehblow, H.D. Speckmann, Corrosion and layer formation of passive copper in alkaline solutions, Werkst. Korros. 35 (1984) 512–519.

[17] B. Miller, Split-ring disk study of the anodic processes at a copper electrode in alkaline solution, J. Electrochem. Soc. 116 (1969) 1675–1680.

[18] H.H. Strehblow, B. Titze, The investigation of the passive behaviour of copper in weakly acid and alkaline solutions and the examination of the passive film by ESCA and ISS, Electrochim. Acta 25 (1980) 839–850.

[19] S.N. Grushevskaya, D.S. Eliseev, A.V. Vvedenskii, Partial currents of anodic oxidation of copper in alkaline media according to rrde data II. Experiment, Prot. Met. Phys. Chem. 53 (2017) 224–230.

[20] E.S. Davydova, F.D. Speck, M.T.Y. Paul, D.R. Dekel, S. Cherevko, Stability limits of Ni-based hydrogen oxidation electrocatalysts for anion exchange membrane fuel cells, ACS Catal. 9 (2019) 6837–6845.

[21] S. Popovic, M. Smiljanic, P. Jovanovic, J. Vavra, R. Buonsanti, N. Hodnik, Stability and degradation mechanisms of copper-based catalysts for electrochemical CO_2 reduction, Angew. Chem. Int. Ed. (2020), https://doi.org/10.1002/anie.202000617.

[22] D. Raciti, M. Mao, J.H. Park, C. Wang, Local pH effect in the CO_2 reduction reaction on high-surface-area copper electrocatalysts, J. Electrochem. Soc. 165 (2018) F799–F804.

[23] T. Burdyny, W.A. Smith, CO_2 reduction on gas-diffusion electrodes and why catalytic performance must be assessed at commercially-relevant conditions, Energy Environ. Sci. 12 (2019) 1442–1453.

[24] O. Kasian, S. Geiger, K.J.J. Mayrhofer, S. Cherevko, Electrochemical on-line ICP-MS in electrocatalysis research, Chem. Rec. 19 (2019) 2130–2142.

[25] M. Schalenbach, O. Kasian, M. Ledendecker, F.D. Speck, A.M. Mingers, K.J.J. Mayrhofer, S. Cherevko, The electrochemical dissolution of noble metals in alkaline media, Electrocatalysis 9 (2017) 153–161.

[26] S. Cherevko, Electrochemical dissolution of noble metals, Reference Module in Chemistry, Molecular Sciences and Chemical Engineering, Elsevier, 2017, pp. 68–75.

[27] V. Shkirskiy, F.D. Speck, N. Kulyk, S. Cherevko, On the time resolution of electrochemical scanning flow cell coupled to downstream analysis, J. Electrochem. Soc. 166 (2019) H866–H870.

[28] A.J. Garza, A.T. Bell, M. Head-Gordon, Is subsurface oxygen necessary for the electrochemical reduction of CO_2 on copper? J. Phys. Chem. Lett. 9 (2018) 601–606.

[29] Y. Lum, J.W. Ager, Stability of residual oxides in oxide-derived copper catalysts for electrochemical CO_2 reduction investigated with (18) O labeling, Angew. Chem. Int. Ed. 57 (2018) 551–554.

[30] D.J.S. Sandbeck, O. Brummel, K.J.J. Mayrhofer, J. Libuda, I. Katsounaros, S. Cherevko, Dissolution of platinum single crystals in acidic medium, ChemPhysChem 20 (2019) 2997–3003.

[31] P.P. Lopes, D. Strmcnik, D. Tripkovic, J.G. Connell, V. Stamenkovic, N.M. Markovic, Relationships between atomic level surface structure and stability/activity of platinum surface atoms in aqueous environments, ACS Catal. 6 (2016) 2536–2544.

[32] S. Geiger, O. Kasian, M. Ledendecker, E. Pizzutilo, A.M. Mingers, W.T. Fu, O. Diaz-Morales, Z.Z. Li, T. Oellers, L. Fruchter, A. Ludwig, K.J.J. Mayrhofer, M.T.M. Koper, S. Cherevko, The stability number as a metric for electrocatalyst stability benchmarking, Nat. Catal. 1 (2018) 508–515.

[33] F.D. Speck, P.G. Santori, F. Jaouen, S. Cherevko, Mechanisms of manganese oxide electrocatalysts degradation during oxygen reduction and oxygen evolution reactions, J. Phys. Chem. C 123 (2019) 25267–25277.

[34] S. Cherevko, Stability and dissolution of electrocatalysts: Building the bridge between model and “real world” systems, Curr. Opin. Electrochem. 8 (2018) 118–125.